# Polarization-Modulated Bent-Core Liquid Crystal Thin Films without Layer Undulation

Cuiyu Zhang, Min Gao, R. R. Ribeiro de Almeida, Wolfgang Weissflog, Oleg D. Lavrentovich, and Antal Jákli

Phys. Rev. Lett. **122**, 137801 — Published 5 April 2019

DOI: 10.1103/PhysRevLett.122.137801

# Polarization-Modulated Bent-Core Liquid Crystal Thin Films Without Layer-Undulation

Cuiyu Zhang[1], Min Gao[1], R.R. Ribeiro de Almeida[1], Wolfgang Weissflog[2],

Oleg D. Lavrentovich[1, 3] and Antal Jákli[1, 3*]

[1]*Chemical Physics Interdisciplinary Program and Advanced Materials and Liquid Crystal Institute, Kent State University, Kent, OH 44242, USA*

[2]*Martin Luther University Halle-Wittenberg, Department of Chemistry, Physical Chemistry, von-Danckelmann-Platz 4, 06120 Halle, Germany*

[3]*Departmnent of Physics, Kent State University, Kent, OH 44242, USA*

**corresponding author: ajakli@kent.edu*

*Spatial confinement is known to affect molecular organizations of soft matter. We present an important manifestation of this statement for thin films of bent-core smectic liquid crystals. Prior freeze fracture transmission electron microscopy (FF-TEM) studies carried out on nitro substituted bent-core mesogens (n-OPIMB-$NO_2$) revealed an undulated smectic layer structure with undulation periodicity ~8 nm. Here we report cryogenic TEM measurements on ~100 nm thick 8-OPIMB-$NO_2$ films. In contrast to FF-TEM results, our studies show only density modulation with periodicity b=16.2nm, and no smectic layer undulation. We show that the discrepancy between the FF-TEM and cryo-TEM results can be attributed to the different sample thicknesses used in the experiments. FF-TEM monitors cracked surfaces of a relatively thick (5-10μm) frozen sample, whereas cryo-TEM visualizes the volume of a thin (0.1μm) film that was quenched from its partially fluid phase. These results have importance in possible photovoltaics and organic electronics applications where submicron thin films are used.*

Nanostructures of thermotropic liquid crystals (LC) in bulk are usually studied by small-angle x-ray scattering (SAXS) or freeze-fracture transmission electron microscopy (FF-TEM) techniques. SAXS reveals electron density variation of bulk samples in about 1 nm to 100 nm range, while FF-TEM images greater than 2 nm surface modulations of replicas made on cracked bulk samples. Recently it was shown that cryogenic transmission electron microscopy (cryo-TEM) can also provide useful and unique nanoscale information even of single compound LCs. [1–4] Cryo-TEM is imaging lateral electron density modulations with about 0.5 nm resolution in films up to about hundred nanometer thickness without the need of replica, therefore monitors the nanostructure of thin films. This is significant, since there are increasing number of applications where liquid crystals are in thin film forms, such as in photovoltaic [5] and organic electronics [6] applications. For example, layer undulations may not be compatible with smooth surfaces, resulting in considerably different nanostructures in thin films than in bulk samples. Consequently, it is vital to compare nanostructures in different conditions, such as monitored by FF-TEM and cryo-TEM.

The polarization modulated tilted smectic phase of bent-core liquid crystals [7] (formerly called B7 [8,9]) phase [10] has extremely interesting nanostructure. In bulk these materials form peculiar micrometer scale helical patterns and slender freely suspended filaments [11–16]. Small angle x-ray scattering (SAXS) studies revealed their complex 2-D scattering profiles [8,10,17] (see Figure 1a) that could be well indexed by a monoclinic 2D unit cell with lattice parameters $a \sim 3\text{-}5\ nm$ and $b \sim 8\text{-}20\ nm$. FF-TEM studies found that the periodicity $b$ is due to layer undulation (*Figure 1*c), which forms to avoid density modulation related to ferroelectric polarization splay and the tilted director structure (*Figure 1*b). [10,18,19] Later it was proposed that for some of these materials the layer undulation is so strong that the layers break into small ribbons, (see Figure 1d) which means that they can be considered as a columnar (originally known as B1 [20]) phase [17]. While in the undulated smectic structures the layers are continuous through the polarization splay defects, in the columnar phase the layers have alternating stepwise half layer thickness displacements. [21] Undulations and the steps-wise displacements are not likely to form adjacent to flat surfaces, therefore it is interesting to study their structures in thin films.

Recently SAXS and cryo-TEM studies of three nitro- substituted (n-OPIMB-$NO_2$, n = 7, 9 and16) bent-core liquid crystals (LCs) were reported. [22] While SAXS studies showed two periodicities between $a_X \sim 3.4–4.7\ nm$ and $b_X \sim 9–16\ nm$ (subscript $X$ refers to data measured by x-ray), cryo-TEM images did not show the layer spacing $a$ but revealed strong transmitted electron intensity modulation with periodicity $b_T \sim b_X\text{-}1nm$, where subscript $T$ means it is measured by TEM. Strangely, the intensity variation was much larger than what a layer undulation model could explain. Additionally, an intensity modulation with a period $c \sim 100–200\ nm$ was also observed (*Figure 1*e). These observations were consistent with a B1-type model where the surface of conformal columns alternates being parallel to two different low-order faces of the lattice as illustrated in the overlaid sketch in *Figure 1*e, although it could not explain the large intensity modulation with periodicity $b_T$.

In this paper we describe cryo-TEM studies of 2-nitro-1,3-phenylenebis[4-(4-octyloxyphenyliminomethyl)benzoate] (8-OPIMB-$NO_2$) that has been extensively studied in bulk form [10,11,16,17,21,23–25]. In contrast to the prior observations on the n=7,9 and 16 homologs described above, here both $a_T=a_X$ and $b_T=b_X$ modulations were found. We also show that in 0.1 μm thin film the density modulation caused by the polarization splay domains (see *Figure 1*b) is not converted to either layer undulations (*Figure 1*c) nor step-wise layer displacements (*Figure 1*d) that were observed by the Boulder group using FF-TEM.

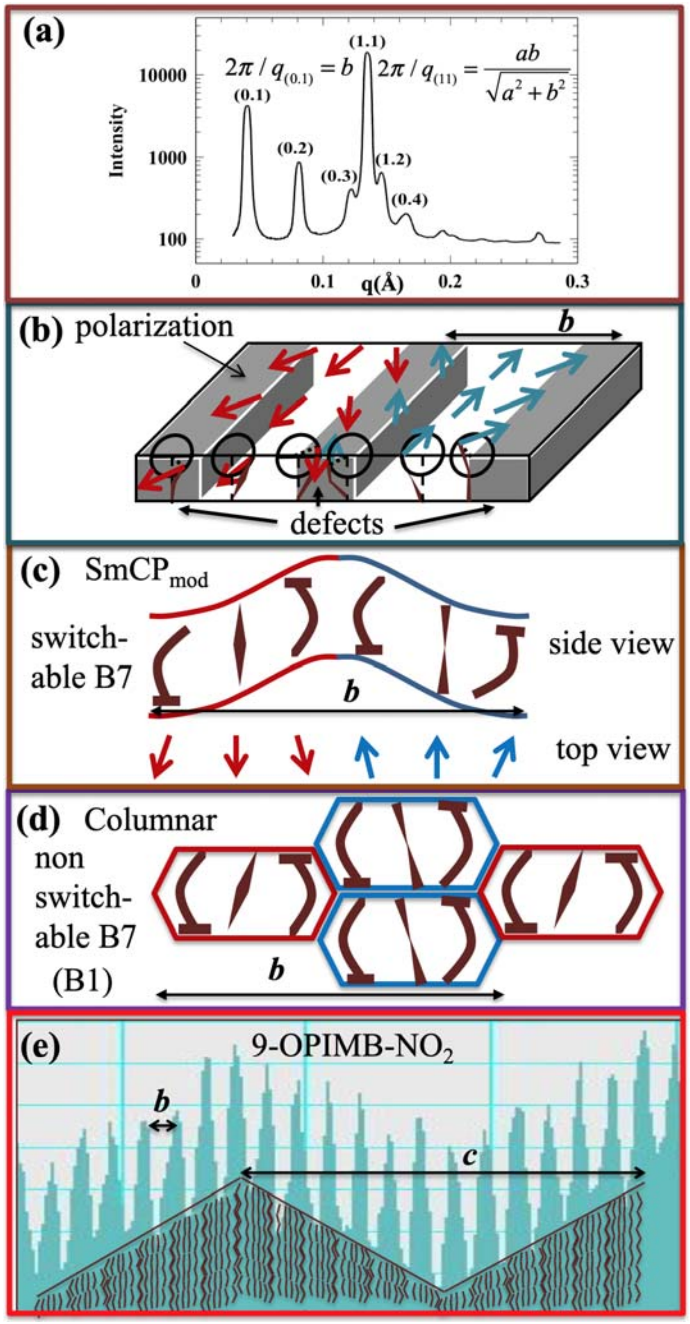


*Figure 1: Summary of the main structural features of the prototype B7 materials. (a) typical q-dependence of small angle x-ray scattering (SAXS) intensity at 150°C; (b) Illustration of the polarization splay and the resulting appearance of periodic defects with lower mass density; (c) Schematics of the undulated layer structure without defects; (d) Columnar structure where the layer undulation is replaced by stepwise displacement of the layers; (e) Transmit-*

*ted electron density profile observed on 9-OPIMB-$NO_2$ at 130$^o$C with overlaid proposed molecular arrangements.*

The molecular structure of 8-OPIMB-$NO_2$ is shown in Figure 2(a). The extended length of the molecule is 4.7 nm. Prior POM studies of 8-PIMP-$NO_2$ revealed formation of typical B7-type helical superstructures starting at 177ºC and above the crystal transition at 116ºC. [8]

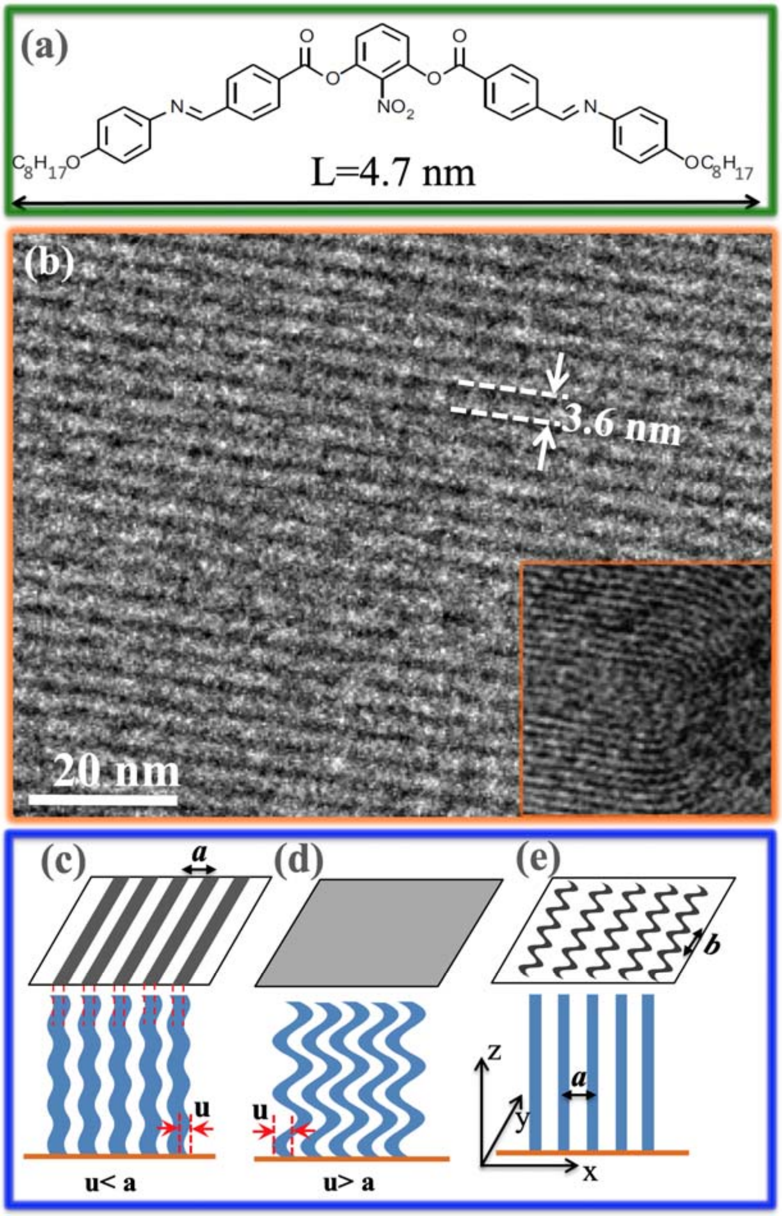


*Figure 2: Molecular structure of the studied 8-OPIMB-$NO_2$ and the appearance of the a=3.6nm stripes. (a) Chemical structure of 8-OPIMB-$NO_2$; (b) cryo-TEM image of an area with stripes of a~3.6nm periodicity corresponding to smectic layer spacing. In the main pane the smectic layers have uniform direction, whereas the inset at the bottom-right shows a defect area where the smectic layers turn around by 180º; (c-e) Illustration of expected TEM*

*images in case of several possible layer undulations:(c) u<a, (d) u>a, (e) u=0 but the smectic layers are modulated in plane normal to the smectic layers.*

Our cryo-TEM studies were carried out with a FEI Tecnai F20 microscope as described in Methods section of Supplemental Information (SI). Our 8-PIMP-$NO_2$ films of 70-100 nm thicknesses were quenched from 150ºC. At this temperature prior x-ray scattering (SAXS) studies [10,17] found electron density modulations with *3.6nm* and *8-9 nm* periodicities that they make an angle $\gamma=81^o$ with each other and was also concluded that this material has a columnar (B1)-type nanostructure, as illustrated in *Figure 1*d. [17] [21]

Representative cryo-TEM textures quenched from 150ºC are seen in Figure 2b, Figure 3a and Figure S-1. Figure 2b shows a cryo-TEM image of an area with stripes of about 3.6nm periodicity, that corresponds to the smectic layer spacing, as found by prior SAXS studies. [10] Notably, in the entire area we cannot see any modulation with *b*=16.2nm periodicity. The observations of the stripes with periodicity equal to the layer spacing requires a difference in the electron densities of the aromatic molecular cores and hydrocarbon tails, and that the layers be perpendicular to the substrate, as illustrated in Figure 2c. [1] Otherwise the electron beam passing through the material normal to the substrates would hit both the core and tail areas, thus wiping out any electron density contrast (Figure 2d). The observation of stripes also excludes the columnar model [17] [21], since in case of stepwise half layer shifts (see *Figure 1*c) the tail and core areas would overlap and would result no fringes with the periodicity of the layer spacing. As we discuss in the Supplementary Information (SI) and show in Figure 2c, the contrast decreases for sinusoidally undulated layers perpendicular to the substrate with the amplitude of the modulation *u*, and becomes smaller than the experimental noise for $u \geq a$ (Figure 2d).

Figure 2e shows an expected TEM image when the axis of the *b=16.2nm* stripes is parallel to the substrates. In this case the *a=3.6nm* stripes should appear undulated with periodicity *b=16.2nm.* Careful inspection of hundreds of TEM images could not reveal any undulated pattern. Additional representative cryo-TEM images are shown in Figure S-1.

Another significant observation is that, in addition to the fairly straight stripes, we found areas where the layers make a 180 degree reorientation in the form of a U-turn (inset in Figure 2b) and the layers' normal experiences pure splay, as dictated by the equidistance of smectic layers. [26] This defect structure not only verifies the layered smectic structure, but also excludes the possibility of any long-range periodic order within the smectic layers in the plane perpendicular to the disclination axis. In other words, if the *b=16.2nm* stripes were present in the structure, they should be aligned horizontally, parallel to the plane of Figure 2b.

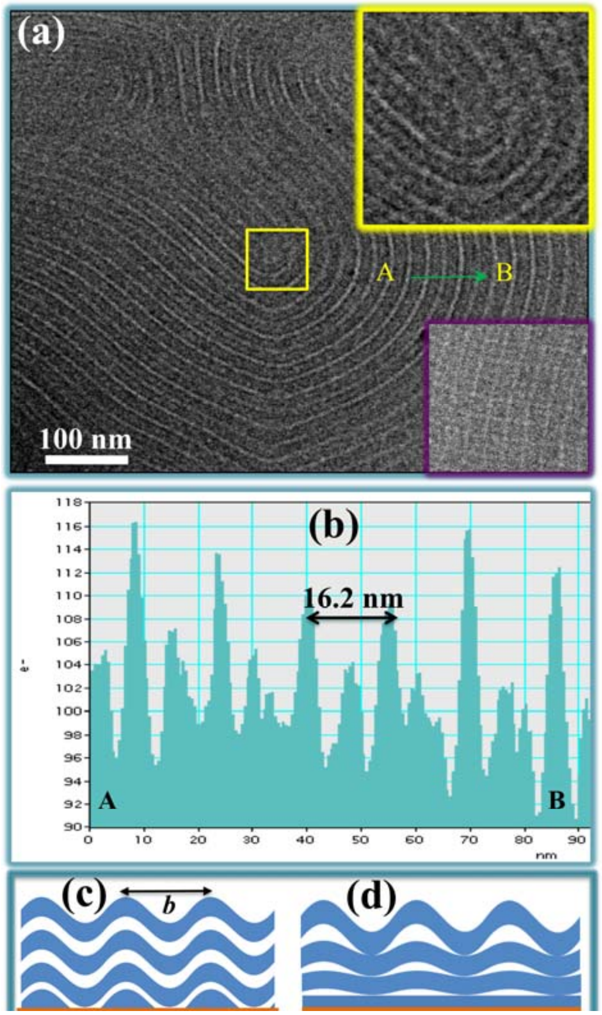


*Figure 3: Summary of cryo-TEM results on an area that shows transmitted electron intensity modulation with periodicity of b=16.2nm. (a) Cryo-TEM image showing a labyrinth structure of b=16.2nm stripes. Inset on the right-bottom corner shows an area with crossing b=16.2nm stripes. (b) The transmitted electron intensity measured along the line from A to B on the main pane of (a). (c and d) Schematic illustration of undulating layers along the substrates: (c) Undulation amplitudes are constant normal to the substrate; (d) undulation amplitude increases normal to the substrate.*

In contrast to Figure 2b, where we see only *a=3.6nm* stripes, Figure 3a shows an area with *b=16.2nm* stripes, which is twice of that found in bulk by SAXS measurements [10,17,27]. In the main pane the stripes follow a labyrinth-type pattern, whereas the inset on the bottom-right corner shows an area of *b=16.2nm* stripes in two coexisting directions. The spatial dependence of the transmitted electron intensity measured across the fringes between A and B on the main pane is shown in Figure 3(b). Although the intensity profile is somewhat noisy (about 30% of the variation $\Delta I_{max}$), it is clearly seen that there is an additional, weaker maxima between the major peaks. This explains why prior x-ray measurements [10,17,27] have detected periodicity with *16.2/2~8 nm*. We estimate (see SI) that the observed intensity modulation would correspond to about 20 nm variation of the film thickness, which is larger than the lateral periodicity *b*. In view of the physical mechanism of layer undulations proposed by Coleman et al. [10], the undulation amplitude should not be larger than $\Delta h_b = \tan\theta \cdot (b/2) \approx b/2$. This shows that the observed *b=16.2nm* stripes cannot be at least fully due to layer undulations. This actually can be expected, since undulated smectic layers running along the flat substrate would be incompatible with the surface, as illustrated in Figure 3(c). As shown in Figure 3(c), layers with constant spacing would necessarily lead to periodic array of defects near the substrate. The appearance of those defects can only be avoided if the layer adjacent to the substrate were not undulated, and the undulation amplitude would increase toward the free surface. In this case, however the layer spacing would need to change (Figure 3d), which has large energy penalty. Accordingly, we conclude that the *b=16.2nm* stripes represent only density modulations without layer undulations (see Figure 2a and Figure 4a), both for layers parallel and perpendicular to the substrates, as evidenced by cryo-TEM results shown in Figure 2b and Figure 3a, respectively. Such a conclusion also explains the large intensity modulations with *b=16.2nm* periodicity observed in films of n=7.9 and 16 homologs of n-PIMB-$NO_2$ (see *Figure 1*e).

The thickness *h* of a film where the undulation is suppressed by the surface, can be estimated by balancing the bulk energy of periodic layers' tilts, approximated as $\frac{1}{2}B\int_0^h\left[\frac{1}{2}\left(\frac{\partial u}{\partial x}\right)^2\right]^2 dz$, and the surface anchoring cost of these tilts that can be written as a quadratic function $\frac{1}{2}W\left(\frac{\partial u}{\partial x}\right)^2$ of the layers' tilt angle $\frac{\partial u}{\partial x}$. Here *B* is the layer compression modulus, $u = u_o \cos(2\pi x/b)$ and *W* is the anchoring strength. The quadratic surface anchoring potential is justified for weakly undulating layers, in which case the sign of the tilt changes periodically along the x-axis [28] Assuming $u_o \le a/2$, and taking into account that in smectic liquid crystals $W = B \cdot a$ [29], we get that $h \ge \frac{16b^2}{a} \simeq 0.4\mu m$. This value is larger than the thickness of our film and smaller than used in FF-TEM measurements, thus appear to explain the differences found between cryo-TEM and FF-TEM.

The labyrinth type pattern of the *b=16.2nm* stripes with $\pm 1/2$ disclinations shows the non-polar character of these stripes (polar stripes could form only integer-strength lines [26]). On the other hand, according to the polarization modulated (PM) model of the B7 phase [10] each stripe is characterized by a polarization splay, with a non-zero net value. The net polarization in subsequent stripes may alternate as shown in Figure 4b, or they can alternate in every other stripes (see Figure 4b). In both cases the net polarization averages to zero within 16 nm that marks the distance between the larger peaks in Figure 3b. That alteration explains the presence of the ½ disclination shown in Figure 3a. The magnified image of the core of the disclination in the upper inset of Figure 3a shows that the contrast associated with the periodic order practically vanishes within an area of a radius $\sim b$, since at the disclination core the positional order is destroyed [26].

The observation that the *b=16.2nm* stripes in the same areas can run in two different directions (lower inset of Figure 3a and Figure S-1(d)) suggests that layers with electron density modulations in different directions overlap. If there were layer undulations, the overlap would lead to empty volumes, which would be energetically costly. Therefore, we assume in the overlapping areas the layers are flat as schematically illustrated in Figure 4b.

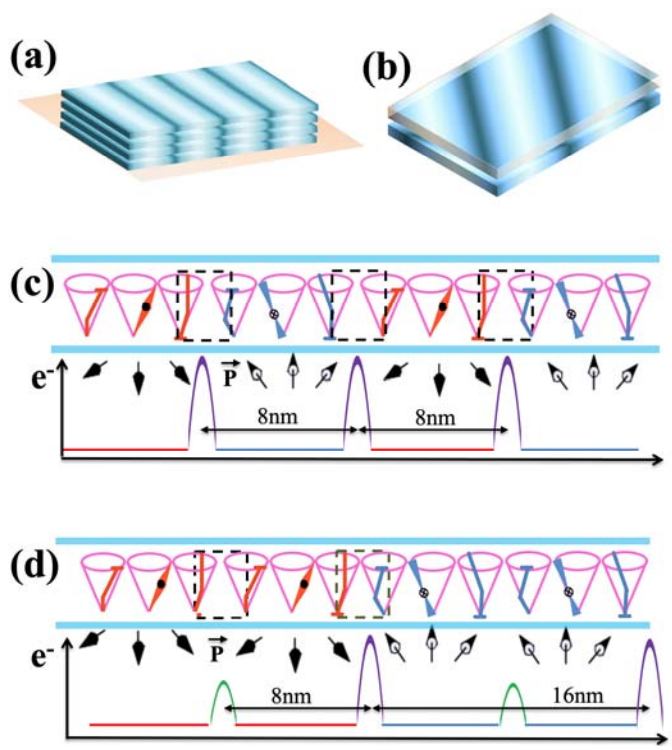


*Figure 4: Proposed models to explain the cryo-TEM images showing area with b=16.2nm stripes. (a) Schematic illustration of flat layers with electron density modulation correspond-*

*ing to a local structure of the main pane in (a); (b) Overlapping sheets of flat smectic layers with electron density modulations in different directions corresponding to the inset of Figure 3a;*
*(c) Model of director structures with polarization splay modulation that would lead to b=16.2nm stripes with single intensity modulation (not corresponding to our experimental observation);(d) Model of director structures with polarization splay modulation that would lead to b=16.2nm stripes with double intensity modulation (corresponding to our experimental observation shown in Figure 2b).*

To find out which of the polarization splay models of Figure 4 we are dealing with, we need to analyze the density variations at the domain boundaries. When the polarization directions in the adjacent splay domains alternate, then both the director tilt and molecular bend directions change sign at the domain boundaries, as shown in Figure 4c and Figure 1(D) of Ref. [10]. That would lead to equal density variations at the domain boundaries leading to a single periodicity. To explain the double periodicity modulation that we found experimentally, we therefore have to assume that the polarization directions are changing signs only in every other polarization splay domain wall, as illustrated in Figure 4d. In that case the density change (and the transmitted electron intensity variation) is smaller when the molecules tilt in the same direction in the neighbor domains, and larger when their tilt directions are opposite at the polarization splay boundary. We note that other local director arrangements, such as doubly tilted $SmC_G$-type structure of the B7 phase [32], could also explain a double periodicity. In that case both the tilt of the molecular planes and the tilt of the director (leaning) would be alternating in adjacent splay domains.

To summarize, the results of our cryo-TEM studies on 8-OPIMB-$NO_2$ are compatible with the polarization modulation model of Coleman et al [10], but does not show the secondary layer undulations that were observed by FF-TEM measurements in several micrometer thick samples. [33] This shows that the layer undulations appearing in bulk as the consequence of the polarization splay can be suppressed in thin films. Our results therefore show that in submicron thin films the nanostructures of certain liquid crystal phases can be different from those observed in bulk or in films with over micrometer thickness. We note that size dependent structures are known in other liquid crystals with periodic structures. For example, in chiral liquid crystals a helical pitch is suppressed in films with thicknesses less than the pitch [30], in helical nanofilament or in twist-bend nematic phase the structure is modified at surfaces. [3], [31] The unusual feature of the suppression of the layer undulation in the $B_7$ phase is the order of magnitude larger thickness range than of the periodicity. The decrease of the density with 8 and 16 nm periodicities would make thin films susceptible for intake of nanoparticles, such as gold, quantum dots or $C_{60}$. The use of $C_{60}$ may have importance in organic photovoltaics to achieve efficient heterojunctions [34]. The modulated environment influences strongly the electric transport properties, as discussed recently. [35]

***Acknowledgement:*** *This work was financially supported by NSF DMR 1307674. The TEM data were obtained at the cryo-TEM facility at the Liquid Crystal Institute, Kent State University supported by the Ohio Research Scholars Program "Research Cluster on Surfaces in Advanced Materials". AJ and ODL are thankful to Noel Clark for sharing their FF-TEM data on the studied material and for useful discussions.*

## References

[1] C. Zhang, M. Gao, N. J. Diorio, W. Weissflog, U. Baumeister, S. N. Sprunt, J. T. Gleeson, and A. Jákli, Phys. Rev Lett. **109**, 107802 (2012).

[2] C. Zhang, B. K. Sadashiva, O. D. Lavrentovich, and A. Jákli, Liq. Cryst. **40**, 1636 (2013).

[3] C. Zhang, N. Diorio, O. D. Lavrentovich, and A. Jákli, Nat. Commun. **5**, 3302 (2014).

[4] M. Gao, Y. K. Kim, C. Zhang, V. Borshch, S. Zhou, H.-S. Park, A. Jákli, O. D. Lavrentovich, M. G. Tamba, G. H. Mehl, D. Studer, B. Zuber, H. Gnägi, and F. Lin, Microsc. Res. Tech. **77**, 754 (2014).

[5] R. A. Callahan, D. C. Coffey, D. Chen, N. A. Clark, G. Rumbles, and D. M. Walba, ACS Appl. Mater. Interfaces **6**, 4823 (2014).

[6] C. M. Keum, S. Liu, A. Al-Shadeedi, V. Kaphle, M. K. Callens, L. Han, K. Neyts, H. Zhao, M. C. Gather, S. D. Bunge, R. J. Twieg, A. Jakli, and B. Lüssem, Sci. Rep. **8**, 699 (2018).

[7] A. Jákli, O. D. Lavrentovich, and J. V. Selinger, Rev. Mod. Phys. **90**, 045004 (2018).

[8] G. Pelzl, S. Diele, A. Jákli, C. H. Lischka, I. Wirth, and W. Weissflog, Liq. Cryst. **26**, 135 (1999).

[9] G. Pelzl, S. Diele, A. Jákli, and W. Weissflog, Liq. Cryst. **33**, 1513 (2006).

[10] D. A. Coleman, J. Fernsler, N. Chattham, M. Nakata, Y. Takanishi, E. Körblova, D. R. Link, R.-F. R. R.-F. Shao, W. G. Jang, J. E. Maclennan, O. Mondainn-Monval, C. Boyer, W. Weissflog, G. Pelzl, L.-C. Chien, J. A. N. Zasadzinski, J. Watanabe, D. M. Walba, H. Takezoe, and N. A. Clark, Science (80-. ). **301**, 1204 (2003).

[11] A. Jákli, D. Krüerke, and G. G. Nair, Phys. Rev. E **67**, 05170201 (2003).

[12] A. Nemeş, A. Eremin, R. Stannarius, M. Schulz, H. Nádasi, and W. Weissflog, Phys. Chem. Chem. Phys. **8**, 469 (2006).

[13] A. Eremin, A. Nemeş, R. Stannarius, M. Schulz, H. Nádasi, and W. Weissflog, Phys. Rev. E **71**, 31705 (2005).

[14] R. Stannarius, A. Nemeş, and A. Eremin, Phys. Rev. E **72**, 020702 (2005).

[15] A. Eremin, U. Kornek, S. Stern, R. Stannarius, F. Araoka, H. Takezoe, H. Nadasi, W. Weissflog, and A. Jakli, Phys. Rev. Lett. **109**, 017801 (2012).

[16] C. A. Bailey and A. Jákli, Phys. Rev. Lett. **99**, 207801 (2007).

[17] C. Folcia, J. Etxebarria, J. Ortega, and M. B. Ros, Phys. Rev. E **72**, 041709 (2005).

[18] N. Vaupotič and M. Čopič, Phys. Rev. E **72**, 031701 (2005).

[19] N. Vaupotič, M. Čopič, E. Gorecka, and D. Pociecha, Phys. Rev. Lett. **98**, 247802 (2007).

[20] G. Pelzl, S. Diele, and W. Weissflog, Adv. Mater **11**, 707 (1999).

[21] D. A. Coleman, C. D. Jones, M. Nakata, N. A. Clark, D. M. Walba, W. Weissflog, K. Fodor-Csorba, J. Watanabe, V. Novotna, and V. Hamplova, Phys. Rev. E **77**, 21703 (2008).

[22] C. Zhang, S. M. Salili, N. Diorio, W. Weissflog, and A. Jákli, Liq. Cryst. **42**, 1621 (2015).

[23] A. Jákli, C. Lischka, W. Weissflog, G. Pelzl, and A. Saupe, Liq. Cryst. **27**, 1405 (2000).

[24] T. Niori, T. Sekine, J. Watanabe, T. Furukawa, and H. Takezoe, J. Mater. Chem. **6**, 1231 (1996).

[25] L. E. Hough, H. T. Jung, D. Krueerke, M. S. Heberling, M. Nakata, C. D. Jones, D. Chen, D. R. Link, J. A. N. Zasadzinski, G. Heppke, J. P. Rabe, W. Stocker, E. Koerblova, D. M. Walba, M. A. Glaser, and N. A. Clark, Science **325**, 456 (2009).

[26] P.-G. de Gennes, *The Physics of Liquid Crystals* (Clarendon Press, Oxford, 1974).

[27] D. A. Coleman, Effects of the Spontaneous Polarization on the Structural and Dynamic Properties of Ferroelectric Liquid Crystals By, University of Colorado at Boulder, 2003.

[28] T. Ishikawa and O. Lavrentovich, Phys. Rev. E **63**, 030501 (2001).

[29] Z. Li and O. D. Lavrentovich, Phys. Rev. Lett. **73**, 280 (1994).

[30] P. G. de Gennes and J. Prost, *The Physics of Liquid Crystals* (Clarendon Press; Second Edition edition, Oxford, 1993).

[31] M. P. Rosseto, R. R. Ribeiro De Almeida, R. S. Zola, G. Barbero, I. Lelidis, and L. R. Evangelista, J. Mol. Liq. **267**, 266 (2018).

[32] A. Jákli, D. Krüerke, H. Sawade, and G. Heppke, Phys. Rev. Lett. **86**, 5715 (2001).

[33] N. A. Clark, *Private Communication* (2014).

[34] N. S. S. Sam-Shajing Sun, editor , *Organic Photovoltaics: Mechanisms, Materials and Devices*, 1. (Taylor and Francis, Boca Raton, FL, 2005).

[35] R. R. Ribeiro de Almeida, L. R. Evangelista, E. K. Lenzi, R. S. Zola, and A. Jákli, Commun. Nonlinear Sci. Numer. Simul. **70**, 248 (2019).